Helium-like atom as a classical three-body problem

T.J.Stuchi[1], A.C.B.Antunes[1] and M.A.Andreu[2]
[1] Instituto de Física, Universidade Federal do Rio de Janeiro,
Caixa Postal 68.528, 21945-970 Rio de Janeiro, RJ, Brazil.
e–mail: tstuchi@if.ufrj.br
[2] Dept. Matemàtica Aplicada i Anàlisi, Univ. Barcelona
Gran Via 585, 08007–Barcelona (Spain)
e–mail: mangel@maia.ub.es

June 23, 1999

Abstract

We study the classical problem of the muonic helium atom, a helium atom with one of its electrons replaced by a muon. Firstly, we establish the connection of the model with the one-dimensional frozen planetary approximation of the helium atom. After that, we find that there is only an equilibrium configuration if the particles are allowed a non-zero angular momentum with the alpha/muon distance restricted. We then present the restricted muonic helium problem, an approximation for the movement of the electron in the potential of the alpha/muon pair moving in a circular orbit. In this model we find that there is only an equilibrium point of the type center-saddle-center. The planar and vertical Lyapunov families of periodic orbits and their stability parameters have been studied showing that the planar family bifurcate into Halo orbits like its gravitational counterpart. The most interesting feature is the stability of these Halo orbits for a range of energy values. The vicinity of the alpha particle is also studied using a Levi–Civita regularization of the electron-alpha particle collision. The movement gets more and more chaotic as the energy increases. However, we find that retrograde zones of bounded stability are possible for energies higher than that of the equilibrium point, when the zero velocity curves open.

1 Introduction

The helium and helium-like atoms are essentially quantum systems. However, a classical approach to these systems may have two motivations which make their analysis worthwhile. The first one is that these systems may be considered as good laboratories for application of the analytical and numerical techniques developed for analyzing dynamical systems. Other reasons for the application of classical methods of analysis to helium and helium-like atoms is that some classical results of these systems may possibly be used to get some insights on the quantized counterpart. A characteristic of these systems which may be obtained by classical methods are the equilibrium points. The determination of the nature of these points concerning the stability may be used to predict the local probability distribution given by the quantization. Only phenomena typically quantic like interferences can not be analyzed by classical methods. Thus, effects of exchange forces can not be considered in this framework.

The helium atom has been object of several classical analysis. Some authors considered the possible equilibrium configurations of the systems ([6],[26]). These configurations are shown to be collinear. Other authors use a purely numerical approach to determine the orbits of the system for several kinds of dynamical configurations [25]. Also the helium-like systems were studied using a numerical approach ([3], [21]) and several dynamical configurations were examined by these authors. In this paper we deal with a muonic helium atom in which one electron is replaced by a muon.

In section 3 we analyze the one and two dimensional cases. The known fixed point of the unidimensional helium atom ([6] and [26]) does not exist for our case. However, in a rotating system of reference, the analysis of the forces present in this system permits to conclude that there is only one possible equilibrium configuration, the collinear one.

The gravitational restricted three body problem (RTBP) has been widely studied for many authors (see for instance [24] and [14]). In a similar way, in section 4 we derive a model with the muon in circular orbit around the alpha particle in a synodical reference system. That is called the restricted muonic helium problem (RMHP). This model has an equilibrium point. Its linear stability and the zero velocity curves (*zvc*) are discussed in section 5.

In section 6 we calculate the planar and vertical Lyapunov periodic orbits associated to the equilibrium point. Like in the gravitational case there is a bifurcation where Halo orbits are produced. The interesting feature is that the latter can be stable for a certain range of energy values. This provides an stable region of the phase space where an electron may remain.

In section 7 we regularize the electron-alpha collision and we present some numerical results, showing that the retrograde orbits are more stable than the direct ones. In fact, there are retrograde KAM tori subsisting for energy values higher than that of the saddle-center point.

2 The full problem in an inertial frame

Consider three particles P_i, $i = 1, 2, 3$, with masses m_i at positions given by $\boldsymbol{r}_i$, with respect to an inertial Cartesian frame (x, y, z) with origin at the center of mass of the system. In this frame we define Jacobi's coordinates as follows:

$$\boldsymbol{\rho}_1 = \boldsymbol{r}_2 - \boldsymbol{r}_1, \qquad \boldsymbol{\rho}_2 = \boldsymbol{r}_3 - \boldsymbol{r}_{12}, \qquad \boldsymbol{r}_{12} = \frac{m_1\boldsymbol{r}_1 + m_2\boldsymbol{r}_2}{m_1 + m_2}, \tag{1}$$

where $\boldsymbol{r}_{12}$ gives the position of the center of mass of the particles P_1 and P_2 (see figure 1).

The kinetic energy $T = \frac{1}{2}\sum_j m_j \dot{\boldsymbol{r}}_j$ expressed in Jacobi's coordinates is given by:

$$T = \frac{1}{2}\mu_{12}\dot{\boldsymbol{\rho}}_1^2 + \frac{1}{2}\mu_3\dot{\boldsymbol{\rho}}_2^2 \tag{2}$$

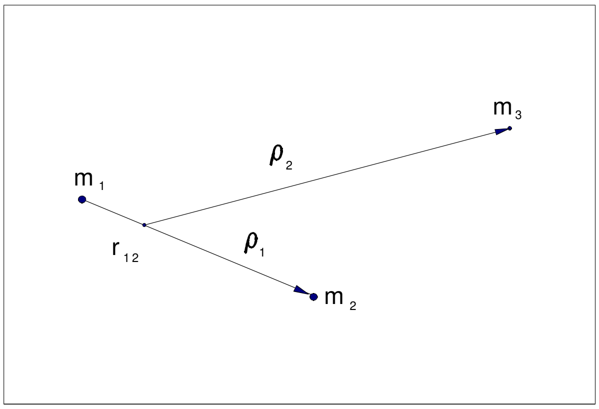

Figure 1: Jacobi's coordinates for three masses.

where the reduced masses are $\mu_{12} = \dfrac{m_1 m_2}{m_1 + m_2}$ and $\mu_3 = \dfrac{m_3(m_1 + m_2)}{m_1 + m_2 + m_3}$. The conjugate momenta to $\boldsymbol{\rho}_1$ and $\boldsymbol{\rho}_2$ are $\boldsymbol{p}_1 = \mu_{12}\dot{\boldsymbol{\rho}}_1$ and $\boldsymbol{p}_2 = \mu_3\dot{\boldsymbol{\rho}}_2$, respectively. For the potential energy we have:

$$V(\boldsymbol{\rho}_1, \boldsymbol{\rho}_2) = V_{12}(\boldsymbol{\rho}_1) + V_{13}(\boldsymbol{\rho}_2 + \frac{m_2}{m_1 + m_2}\boldsymbol{\rho}_1) + V_{23}(\boldsymbol{\rho}_2 - \frac{m_1}{m_1 + m_2}\boldsymbol{\rho}_1) \ , \tag{3}$$

so that the energy of the system is $H(\boldsymbol{\rho}_1, \boldsymbol{\rho}_2, \boldsymbol{p}_1, \boldsymbol{p}_2) = T + V$.

Now, we take P_1, P_2 and P_3 as alpha, muon and electron particles with charges $Q_1 = 2e$ and $Q_2 = Q_3 = -e$, so that we have the classical configuration of a helium like atom. The used values of the masses are $m_\alpha = m_1 = 4.002602u$, $m_\mu = m_2 = .110303035u$, $m_e = m_3 = 5.485799\ 10^{-4}u$ and $u = 931.49432\frac{Mev}{c^2}$, where u stands for the unit of atomic mass.

The only forces acting on the particles are their mutual Coulombian attraction or repulsion. This is the main dynamical difference from the gravitational three-body, where the forces depend only on the masses and they are always attractive. In our case, we will even neglect the gravitational forces since they are much smaller than the Coulombian ones.

We then have that the general form of the Hamiltonian is

$$H(\boldsymbol{\rho}_1, \boldsymbol{\rho}_2, \boldsymbol{p}_1, \boldsymbol{p}_2) = \frac{\boldsymbol{p}_1^2}{2\mu_{12}} + \frac{\boldsymbol{p}_2^2}{2\mu_3} + e^2\left[-\frac{2}{|\boldsymbol{\rho}_1|} - \frac{2}{\left|\boldsymbol{\rho}_2 + \frac{m_2}{m_1+m_2}\boldsymbol{\rho}_1\right|} + \frac{1}{\left|\boldsymbol{\rho}_2 - \frac{m_1}{m_1+m_2}\boldsymbol{\rho}_1\right|}\right] \ . \tag{4}$$

The associated Hamiltonian equations are

$$\dot{\boldsymbol{p}}_i = -\frac{\partial H}{\partial \boldsymbol{\rho}_i}, \quad \dot{\boldsymbol{\rho}}_i = \frac{\partial H}{\partial \boldsymbol{p}_i}, \quad \text{for } \ i = 1, 2 \ . \tag{5}$$

This system has 6 degrees of freedom and its phase space has dimension twelve since we have already used the integrals of the center of mass. The only constants of motion left are now the Hamiltonian itself and the angular momentum which reduces the phase space dimension to eight, a four degrees of freedom problem. We start dealing with the planar case to gain some insight on its dynamical properties.

3 Planar motion

We take ϕ and ψ as the angles made by $\boldsymbol{\rho}_1$ and $\boldsymbol{\rho}_2$ with the x direction, respectively, and $\hat{\boldsymbol{\rho}}_1, \hat{\boldsymbol{\phi}}, \hat{\boldsymbol{\rho}}_2, \hat{\boldsymbol{\psi}}$ the associated orthonormal basis. The momenta can be written as:

$$p_1 = \mu_{12}\dot{\rho}_1, \quad p_\phi = \mu_{12}\rho_1^2\dot{\phi}, \quad p_2 = \mu_3\dot{\rho}_2, \quad p_\psi = \mu_3\rho_2^2\dot{\psi}, \tag{6}$$

so that the kinetic energy is

$$T(\rho_1, \phi, \rho_2, \psi, p_1, p_\phi, p_2, p_\psi) = \frac{1}{2\mu_{12}}(p_1^2 + \frac{p_\phi^2}{\rho_1^2}) + \frac{1}{2\mu_3}(p_2^2 + \frac{p_\psi^2}{\rho_2^2}) \ . \tag{7}$$

The potential energy expressed in terms of $\theta = \psi - \phi$ becomes:

$$\begin{aligned} V(\rho_1, \rho_2, \theta) = \;& e^2 \Bigg(-\tfrac{2}{\rho_1} - 2\left[\rho_2^2 + \left(\tfrac{m_2\rho_1}{m_1+m_2}\right)^2 + \tfrac{2m_2}{m_1+m_2}\rho_1\rho_2\cos\theta\right]^{-1/2} + \\ & + \left[\rho_2^2 + \left(\tfrac{m_1\rho_1}{m_1+m_2}\right)^2 - \tfrac{2m_1}{m_1+m_2}\rho_1\rho_2\cos\theta\right]^{-1/2}\Bigg) \end{aligned}$$

and the constants of motion are obviously $H = T + V$ and angular momentum $L = \mu_{12}\rho_1^2\dot{\phi} + \mu_3\rho_2^2\dot{\psi}$.

3.1 The unidimensional problem

Firstly, we study the possibility of existence of stable unidimensional configurations, that is, $L = \mu_{12}\rho_1^2\dot{\phi} + \mu_3\rho_2^2\dot{\psi} = 0$. The electron and muon are revolving in opposite directions and the problem is reduced to two degrees of freedom. In the case of helium atom for initial conditions alpha–electron–electron there are an equilibrium position for this situation which is known as the frozen planetary approximation (FPA) (see [6] and [26]). We investigate the possibility of such an approximation for the muonic helium.

The Hamiltonian can be obtained from (4) and it is

$$H(\rho_1, \rho_2, p_1, p_2) = \frac{p_1^2}{2\mu_{12}} + \frac{p_2^2}{2\mu_3} + e^2\left[-\frac{2}{|\rho_1|} - \frac{2}{\left|\rho_2 + \frac{m_2}{m_1+m_2}\rho_1\right|} + \frac{1}{\left|\rho_2 - \frac{m_1}{m_1+m_2}\rho_1\right|}\right] \ . \tag{8}$$

The collision alpha-muon has been regularized following in the same way which will be explained in section 7. Different values of the mass m_2 have been considered, from the mass of the m_e to the mass of the muon m_μ. For each value of the mass m_2, integrating the regularized Hamiltonian equations, Poincaré sections for $\{\rho_1 = 0,\ p_1 > 0\}$ have been computed. Figure 2 shows one of these sections for the particle with $m_2/m_e = 30$; the periodic orbit which corresponds to the FPA is at 6.3, and it bifurcates to an unstable orbit around $m_2/m_3 = 35$. Therefore, the system alpha-muon-electron, $m_2/m_3 > 200$, do not have this unidimensional stable configuration.

3.2 Circular orbits

Since we have seen that there are not equilibria configurations in an inertial reference frame, we are going to investigate if there are collinear equilibria with respect to a rotating frame

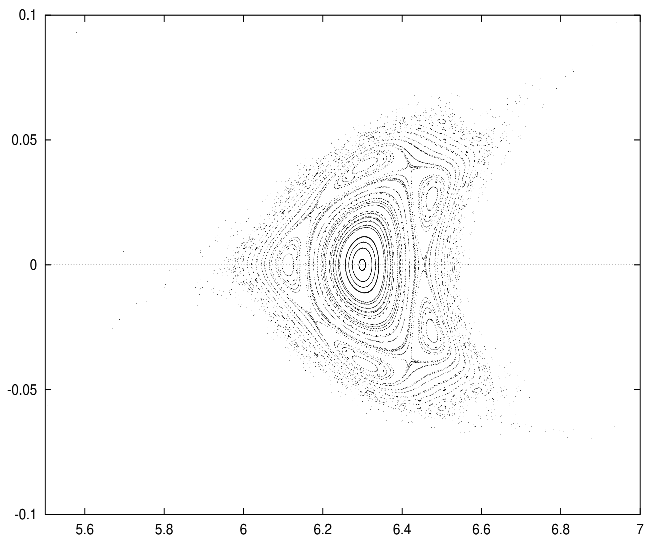

Figure 2: Poincaré section $E = -1$, $\rho_1 = 0$ and $p_1 > 0$ for the one dimensional atom with mass parameter $m_2/m_3 = 30$ where a helium-like stable periodic orbit is shown.

with angular velocity ω. That is circular orbits for the three particles in a inertial frame of reference.

We now search for collinear equilibria, and for such we make $\theta = 0$, $\psi = \phi$, or $\theta = \pi$, $\psi = \phi + \pi$. In this case $\omega = \dot{\phi} = \dot{\psi}$ is the common angular frequency. From the conservation of angular momentum we have $L/\omega = \mu_{12}\rho_1^2 + \mu_3\rho_2^2$, and can take $\rho_2^2 = \frac{1}{\mu_3}\left(\frac{L}{\omega} - \mu_{12}\rho_1^2\right)$ to express both ρ_2 and $\dot{\rho}_2$ in terms of ρ_1 and $\dot{\rho}_1$ in the above Hamiltonian. The new Hamiltonian for the collinear motion is:

$$H = \frac{\omega L}{2} + \frac{1}{2\mu_{12}}\left(1 + \frac{\mu_{12}}{\mu_3}\left(\frac{\rho_1}{\rho_2}\right)^2\right) p_1^2 + V_\pm(\rho_1) \tag{9}$$

with

$$V_\pm(\rho_1) = Q^2\left[-\frac{2}{\rho_1} - 2\left|\rho_2 \pm \frac{m_2}{m_1+m_2}\rho_1\right|^{-1} + \left|\rho_2 \mp \frac{m_1}{m_1+m_2}\rho_1\right|^{-1}\right], \tag{10}$$

where ρ_2 takes the value mentioned above, and the indices $\pm$ stands for $cos\theta = \pm 1$.

The singularities of the potential are $\rho_1 = 0$ and $\rho_1^j = \left[\frac{L}{\omega\mu_3}\left(\frac{\mu_{12}}{\mu_3} + \frac{m_j^2}{(m_1+m_2)^2}\right)^{-1}\right]^{1/2}$, where $j = 1, 2$. If $\rho_1 = 0$, we have the maximum value of ρ_2, $\rho_{2max} = \sqrt{\frac{L}{\omega\mu_3}}$, and conversely, if $\rho_2 = 0$, then $\rho_{1max} = \sqrt{\frac{L}{\omega\mu_{12}}}$.

For the case of a muon there is only one equilibrium, found for V_-, i.e., when $\theta = \pi$. Its value is $\rho_{1e} = 0.94003773$ which corresponds to $\rho_{2e} = 4.77137698$ in units of ρ_{1max}. At this point the second derivative of the potential is negative, a maximum, which means an unstable fixed point.

The equilibrium position of the electron, ρ_{2e}, being reasonably far away from the pair alpha–muon allow us to look at the problem of an electron moving in the potential created by the pair revolving about their common center of mass. Of course, this approximation becomes better for motions of the electron around and besides this position. However, numerical tests show that the approximation is acceptable under less astringent requirements. In the next section we study the reduction to a restricted three-body Coulombian problem in synodic coordinates.

4 The restricted muonic helium problem

Suppose that the alpha and muon particles are moving in circular orbits around their center of mass. We are going to derive the equations of motion of an electron under the Coulombian forces of the alpha muon pair. This restricted muonic helium problem (RMHP) approximation of the full problem has to be handled with care. On the other hand, the full problem may be written as a RMHP plus perturbations. That would allow to obtain orbits of the full problem by means of continuation technics.

Moreover, in this approximation, we essentially assume that the motion of the electron does not disturb the uniform circular motion of the muon around the Helium nucleus. A sufficient condition for the validity of this assumption is that the distance of the electron to the alpha particle is much larger than the alpha–muon distance. The sufficiency of this condition can be evaluated comparing the position of the equilibrium point given by the exact solution in section 3 and the approximate calculation of next section. The relative error is 0.0045648.

Another circumstance in which the approximate description may be used is in some cases of a very rapid passage of the electron near the alpha particle. It can be shown that if the time of interaction is sufficiently small, the impulse transmitted by the electron to the muon may be neglected.

We considered very elongated orbits of the electron along the negative x axis, turning around the alpha particle in the rotating frame. The recoil velocity of the muon in the x direction ($v_{\mu x}$), due to the electron impulse, is compared with the muon velocity in the circular orbit of the inertial frame ($v_{\mu c}$). The relation $v_{\mu x}/v_{\mu c}$ is energy dependent, as can be seen in the table below.

$-E$	36	38	40	70	100
$v_{\mu x}/v_{\mu c}$	0.11	0.049	0.030	0.013	0.001

By inspection, we see that for energies lower than $E = -40.0$ the impulse of the electron on the muon becomes neglible. These calculations were done using the regularization described in section 7. We proceed now to present the RMHP.

To derive the equations of the RMHP we find first the parameters of the circular motion of the muon around the alpha particle. This is a two body problem. Consider an inertial reference frame with the origin in the center of mass. Let $\boldsymbol{r}_1$ and $\boldsymbol{r}_2$ the vector positions of the masses m_1 and m_2 which are the masses of the alpha and muon particles, respectively.

The relative position is denoted by $\boldsymbol{\rho} = \boldsymbol{r}_2 - \boldsymbol{r}_1$. We also have

$$\boldsymbol{r}_1 = \frac{-\mu}{m_1}\boldsymbol{\rho} \; , \qquad \boldsymbol{r}_2 = \frac{\mu}{m_2}\boldsymbol{\rho} \; ,$$

where the mass parameter is $\mu = \frac{m_1 m_2}{m_1+m_2}$. The charges of the alpha and muon particles are $Q_1 = 2e$ and $Q_2 = -e$, respectively. Defining as ϕ the angle of $\boldsymbol{\rho}$ with the x direction, the energy of the system can be written as

$$E = \frac{1}{2}\mu(\dot{\rho}^2 + \rho^2\dot{\phi}^2) - \frac{2e^2}{\rho} \; . \tag{11}$$

Taking into account the conservation of the angular momentum of the system, $L = \mu\rho^2\dot{\phi}$, the expression of the effective potential is given by

$$V_{ef} = \frac{L^2}{2\mu\rho^2} - \frac{2e^2}{\rho} \; . \tag{12}$$

The radius of the circular orbit, ρ_{cir}, is the solution of $\frac{dV_{ef}(\rho)}{d\rho} = 0$. This radius and its corresponding angular velocity are

$$\rho_{cir} = \frac{L^2}{2\mu e^2} \; , \qquad \omega = \frac{4\mu e^4}{L^3} \; .$$

So, they satisfy the relationship

$$\omega^2\rho_{cir}^3 = \frac{2e^2}{\mu}, \tag{13}$$

similar to the third Kepler's law.

We now take a frame centered in the center of mass, rotating with the constant angular velocity ω and with the x axis having the direction of ρ. Here, the mass of the electron is denoted by m and its position is $\boldsymbol{r}$. In this system the equation of motion for the electron is

$$m\frac{d^2\boldsymbol{r}}{dt^2} = \mathbf{F}_1 + \mathbf{F}_2 - m\boldsymbol{\omega} \times (\boldsymbol{\omega} \times r) - 2m\boldsymbol{\omega} \times \frac{d\boldsymbol{r}}{dt} \; , \tag{14}$$

where $\boldsymbol{\omega} = \omega\hat{\mathbf{z}}$ and the Coulombian forces of the alpha and the muon on the electron are given by

$$\mathbf{F}_1 = -2e^2\frac{\boldsymbol{r} - \boldsymbol{r}_1}{|\boldsymbol{r} - \boldsymbol{r}_1|^3} \; , \qquad \mathbf{F}_2 = e^2\frac{\boldsymbol{r} - \boldsymbol{r}_2}{|\boldsymbol{r} - \boldsymbol{r}_2|^3} \; , \tag{15}$$

where $\boldsymbol{r}_1 = x_1\hat{\mathbf{x}}$, $\boldsymbol{r}_2 = x_2\hat{\mathbf{x}}$ with $x_1 = -\frac{\mu}{m_1}\rho_{cir}$ and $x_2 = \frac{\mu}{m_2}\rho_{cir}$. Expressing (14) in the Cartesian rotating coordinates, we get

$$\begin{aligned}
\ddot{x} &= -\frac{e^2}{2m}\left[\frac{2(x-x_1)}{r_1^3} - \frac{x-x_2}{r_2^3}\right] + \omega^2 x + 2\omega\dot{y} \; , \\
\ddot{y} &= -\frac{e^2}{2m}\left[\frac{2}{r_1^3} - \frac{1}{r_2^3}\right] y + \omega^2 y - 2\omega\dot{x} \; , \\
\ddot{z} &= -\frac{e^2}{2m}\left[\frac{2}{r_1^3} - \frac{1}{r_2^3}\right] z \; ,
\end{aligned} \tag{16}$$

where $r_i^2 = (x - x_i)^2 + y^2 + z^2$, for $i = 1, 2$. To use adimensional coordinates we perform the change

$$\begin{array}{ll} X_1 = x_1/\rho_{cir}, & X_2 = x_2/\rho_{cir} \ , \\ \mathbf{R} = \boldsymbol{r}/\rho_{cir}, & \tau = \omega t \ . \end{array}$$

Denoting the variables with low cases again, we have the following set of equations:

$$\begin{aligned} \ddot{x} - 2\dot{y} = \frac{\partial V}{\partial x} &= -\frac{\bar{\mu}}{2}\left[\frac{2(x - x_1)}{r_1^3} - \frac{x - x_2}{r_2^3}\right] + x \ , \\ \ddot{y} + 2\dot{x} = \frac{\partial V}{\partial y} &= \left[1 - \frac{\bar{\mu}}{2}\left(\frac{2}{r_1^3} - \frac{1}{r_2^3}\right)\right] y \ , \\ \ddot{z} = \frac{\partial V}{\partial z} &= -\frac{\bar{\mu}}{2}\left[\frac{2}{r_1^3} - \frac{1}{r_2^3}\right] z \ , \end{aligned} \tag{17}$$

where the derivatives are now with respect to the adimensional time τ. Moreover, we have introduced the parameter $\bar{\mu} = \frac{\mu}{m} = 195.6777175$, for the present values. We want to note that the relationship (13) has been used in the derivation of the equations (17). The potential function is then defined as

$$V(x, y, z) = \frac{\bar{\mu}}{2}\left[\frac{2}{r_1} - \frac{1}{r_2}\right] + \frac{1}{2}(x^2 + y^2) \ . \tag{18}$$

This system has a integral of motion similar to the Jacobi integral for the RTBP:

$$C_J = 2V - (\dot{x}^2 + \dot{y}^2 + \dot{z}^2) \ , \tag{19}$$

C_J being the Jacobi constant of motion. Therefore, we can write a Hamiltonian for the system

$$H(\mathbf{q}, \mathbf{p}) = \frac{1}{2}(p_x^2 + p_y^2 + p_z^2) + y p_x - x p_y - \bar{\mu}\left[\frac{1}{r_1} - \frac{1}{2r_2}\right] \ , \tag{20}$$

with $\mathbf{q} = (x, y, z)$ and $\mathbf{p} = (p_x, p_y, p_z)$. The conjugate momenta are expressed by $p_x = \dot{x} - y$, $p_y = \dot{y} + x$ and $p_z = \dot{z}$, and therefore the Coriolis potential appears rather then the centrifugal potential. We notice that the value of the Hamiltonian function is $-C_J/2$.

The corresponding Hamilton's equations can be easily derived and they are:

$$\begin{aligned} \dot{x} &= p_x + y \ , \\ \dot{y} &= p_y - x \ , \\ \dot{z} &= p_z \ , \\ \dot{p}_x &= p_y - \bar{\mu}\left[\frac{x - x_1}{r_1^3} - \frac{x - x_2}{2r_2^3}\right] \ , \\ \dot{p}_y &= -p_x - \bar{\mu}\left[\frac{1}{r_1^3} - \frac{1}{2r_2^3}\right] y \ , \\ \dot{p}_z &= -\bar{\mu}\left[\frac{1}{r_1^3} - \frac{1}{2r_2^3}\right] z \ . \end{aligned} \tag{21}$$

These equations present two symmetries:

$$S_1 : (x, y, z, \dot{x}, \dot{y}, \dot{z}, t) \longleftrightarrow (x, y, -z, \dot{x}, \dot{y}, -\dot{z}, t) \ , \tag{22}$$

$$S_2 : (x, y, z, \dot{x}, \dot{y}, \dot{z}, t) \longleftrightarrow (x, -y, z, -\dot{x}, \dot{y}, -\dot{z}, -t) \ . \tag{23}$$

The equations of the RTBP present also the same symmetries S_1 and S_2. They are useful for looking for periodic orbits.

5 Fixed points and their linear stability

We can find the fixed points of system (17) taking $V_x = V_y = V_z = 0$, i.e., the partial derivatives of the potential-like function equals to zero, as well as $\dot{x} = \dot{y} = \dot{z} = 0$, or, equivalently, as the equilibrium positions of the Hamiltonian vector field. Both lead to the following set of equations for the configurations variables:

$$x - \frac{\bar{\mu}(x - x_1)}{r_1^3} + \frac{\bar{\mu}(x - x_2)}{2r_2^3} = 0 \; , \tag{24}$$

$$\left(1 - \bar{\mu}\left[\frac{1}{r_1^3} - \frac{1}{2r_2^3}\right]\right) y = 0 \; , \tag{25}$$

$$-\bar{\mu}\left[\frac{2}{r_1^3} - \frac{1}{r_2^3}\right] z = 0 \; . \tag{26}$$

A careful inspection of the above equations shows that the only solutions are for $y = z = 0$. This means that the equilibrium points, if there is any, are collinear. For them, the previous system is reduced to the equation (24).

Then, one can look for an equilibrium point on the left of the alpha particle, between the alpha and the muon, or on the right of the muon particle. Each case leads to a quintic equation which has to be solved numerically. It is easy to see that only the first case is possible. To look for solutions in the negative axis to the left of the α particle, we call $\xi = r_1 = x_1 - x$, then $r_2 = x_2 - x = 1 + \xi$ and $x = x_1 - \xi$. The equation (24) becomes

$$\xi - x_1 - \frac{\bar{\mu}}{\xi^2} + \frac{\bar{\mu}}{2(1+\xi)^2} = 0 \; , \tag{27}$$

and we obtain the quintic equation:

$$2\xi^5 + 2(2 - x_1)\xi^4 + 2(1 - 2x_1)\xi^3 - (2x_1 + \bar{\mu})\xi^2 - 4\bar{\mu}\xi - 2\bar{\mu} = 0 \; . \tag{28}$$

Using $x_1 = -0.026818770$, $x_2 = 0.97318123$ and $\bar{\mu} = 195.6777175$, the positive solution of the equation (28) gives the equilibrium point at $x_0 = -5.05255973$. Note that this solution is quite close to the value we found in the full problem (see section 3.2).

Figure 3 shows the zero velocity curves of the RMHP. In this figure, the saddle$\times$center character (on the xy-plane) of the equilibrium point is visible. The energy of the equilibrium point is $h_0 = -35.46246013$. For lower values of the energy the Hill regions are bounded around the alpha particle. Conversely, for values of the energy higher than h_0 the Hill regions are unbounded.

We shall now examine the linear approximation in a neighborhood of the equilibrium

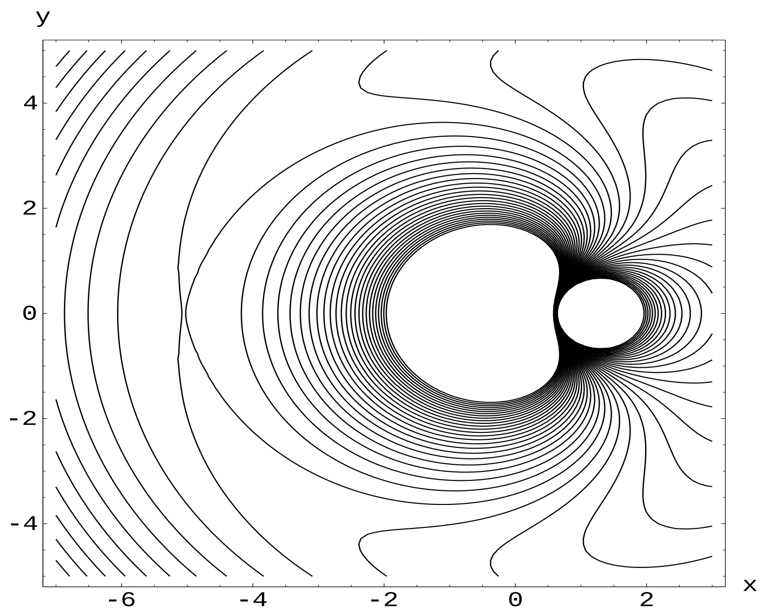

Figure 3: The zero velocity curves of the RMHP. The inner closed curves on the left allow bounded motion around the alpha particle; the right hand closed curves are the repulsive barrier of the muon.

point. The linearization of the equations (21) around the equilibrium point is

$$\begin{pmatrix} \dot\eta_1 \\ \dot\eta_2 \\ \dot\eta_3 \\ \dot\eta_4 \\ \dot\eta_5 \\ \dot\eta_6 \end{pmatrix} = \begin{pmatrix} 0 & 1 & 0 & 1 & 0 & 0 \\ -1 & 0 & 0 & 0 & 1 & 0 \\ 0 & 0 & 0 & 0 & 0 & 1 \\ 2a & 0 & 0 & 0 & 1 & 0 \\ 0 & -a & 0 & -1 & 0 & 0 \\ 0 & 0 & -a & 0 & 0 & 0 \end{pmatrix} \begin{pmatrix} \eta_1 \\ \eta_2 \\ \eta_3 \\ \eta_4 \\ \eta_5 \\ \eta_6 \end{pmatrix} , \tag{29}$$

where

$$a = \frac{\bar\mu}{(x_1 - x_0)^3} - \frac{\bar\mu}{(x_2 - x_0)^3} .$$

The eigenvalues of this system are $\pm 1.07890596i$, ± 0.50828318 and $\pm 1.04609451i$, showing that the equilibrium point is a center$\times$saddle$\times$center. We also want to comment that performing a linear symplectic change of variables, $\eta = S\zeta$ it is possible to express the Hamiltonian of the system (29) as

$$H_2 = \frac{1.07890596}{2}(\zeta_1^2 + \zeta_2^2) + 0.50828318\zeta_3\zeta_4 + \frac{1.04609451}{2}(\zeta_5^2 + \zeta_6^2) . \tag{30}$$

6 Lyapunov and Halo orbits

In the previous section, the linear stability of the equilibrium point has been discussed. The knowledge of periodic orbits is important for some semi-classical methods and leads to promising results ([5], [6], [7], [12] and [16]). We now present the periodic orbits around that point. The Hamiltonian system (21) has two families of periodic orbits emanating from the equilibrium point. Each family corresponds to one of the harmonic oscillators of the linearized system (29). These families of orbits are usually called Lyapunov orbits [17].

The problem of finding a periodic orbit is reduced to look for a fixed point of the Poincaré map defined by the flow of (21) through a transversal section. In our case, we have used the section $\{y = 0\}$. Figure 4a shows several orbits of the planar Lyapunov family. The dashed orbit is the bifurcating orbit where the Halo families start. Later on, we will talk about these families. We notice that as Lyapunov orbits grow and approach collision they move to the right. The orbits can be parameterized by the x coordinate of the crossing point at the section $\{y = 0\}$, on the right of the equilibrium point. The symmetry of the orbits with respect to the cross section is consequence of the symmetry (23). A continuation method (also called homotopy method) has been used to follow the periodic orbits along the family (for more details about the numerical methods see [23] and [18]).

To study the linear stability of each orbit, its monodromy matrix has been used. The monodromy matrix is obtained integrating the variational equations along the orbit. Since the Hamiltonian character of the system, the (eventually complex) eigenvalues of the monodromy matrix are of the form λ_1, $1/\lambda_1$, λ_2, $1/\lambda_2$, apart from 1 with multiplicity 2. The stability parameters are defined as $s_k = \lambda_k + 1/\lambda_k$, for $k = 1, 2$. An orbit is lineary stable if its stability parameters are real and their absolute values are less than 2.

Figure 4b shows the evolution of the stability parameters along the family of planar Lyapunov orbits. The orbits nearby the equilibrium point are elliptic-hyperbolic. The hyperbolic directions are on the xy plane, while the elliptic one corresponds to the z coordinate. The bifurcation of the Halo occurs when there is a change from stable to unstable in the Lyapunov family in the z direction.

Figure 5 shows several orbits of the vertical Lyapunov family of periodic orbits. They are called vertical because they start from the equilibrium point in the direction of the z coordinate and they are very narrow in the x and y directions. Sometimes, they are also called the eight shaped family. As far as we have followed this family, all the orbits are elliptic-hyperbolic.

Another way to understand why the bifurcation of the Halo orbits takes place is the following one. We recall that we have seen in section 5 that the equilibrium point has two different frequencies, but they are quite close. Following the family of planar Lyapunov orbits, the frequency (or the period, if you prefer) varies. Moreover, the frequency in the vertical direction also varies along this family. The bifurcation of the Halo occurs when the frequency of the Lyapunov orbit coincide with the frequency in the vertical direction. There, two families of Halo orbits are born. These families are symmetric with respect to the xy plane because of the symmetry (22).

Figure 6a shows the evolution of the one of the Halo families (xz projection). The dotted line is the maximum and minimum value of z reached by them. The two diamonds show the position of the muon and alpha particles. Figure 6b shows the (y, z) projection of some of these orbits. Figure 6c is a magnification of 6a.

The evolution of the stability parameter since the bifurcation up to the maximum z value reached by the Halo orbits is shown in Figure 6d. The continuous line represents real stability parameters, s_1 and s_2. In regions where they are complex conjugate we show the

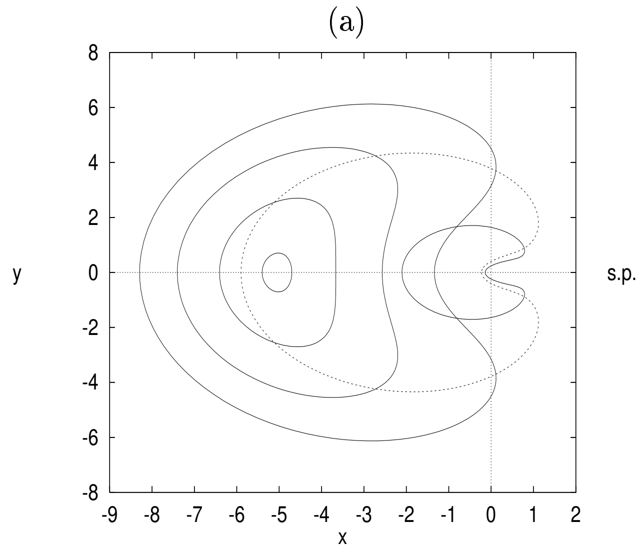

Figure 4: a) The family of planar Lyapunov periodic orbits. The broken line is the bifurcating orbit from which Halo orbits appear. b) Stability parameters of this family.

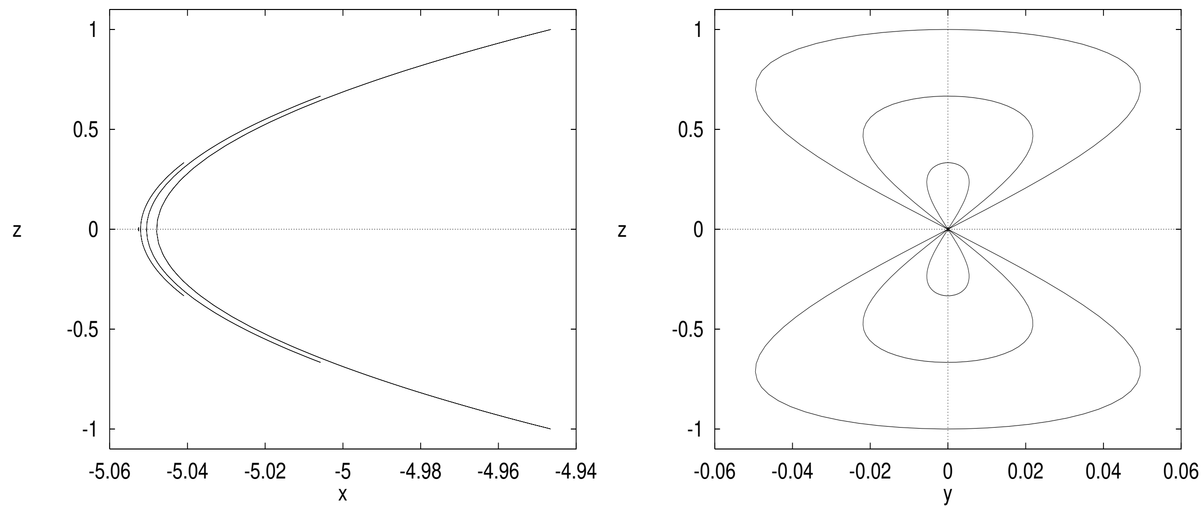

Figure 5: The vertical Lyapunov orbits which like in the RTBP are "eight" shaped. From left to right, xz and yz projections. Notice that these orbits are very narrow in the x and y directions.

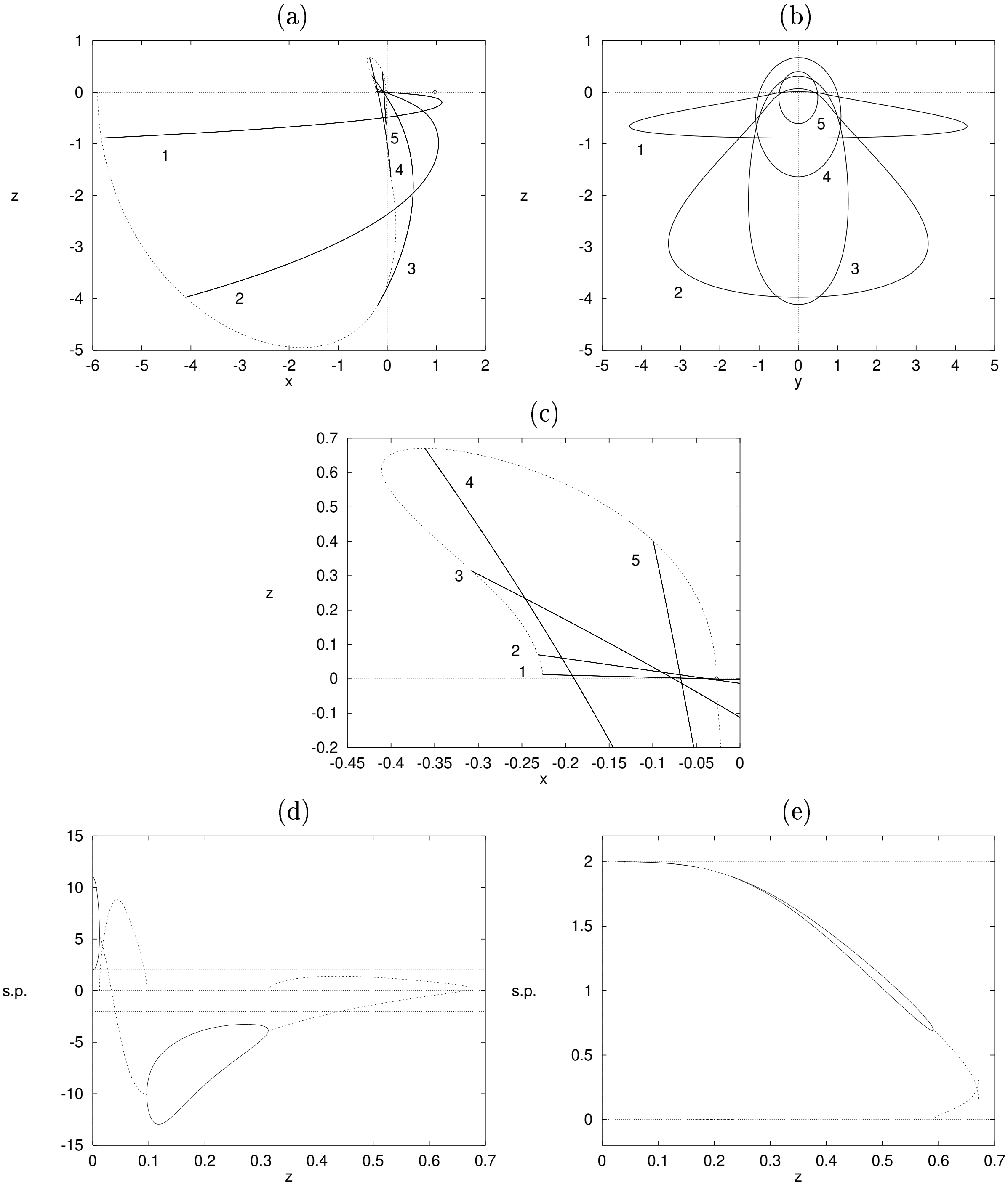

Figure 6: a) The evolution of the Halo orbits in the xz projection; b) the yz projection; c) Magnification of part of a). d) Evolution of the stability parameters since the bifurcation up to the orbit with maximum z; e) Continuation of the stability parameters from z maximum towards the alpha particle. The orbits $z \in (.233, .591)$ and $z < 0.16$ are all stable.

real and imaginary part of s_1 with a discontinuous line. After the z-maximum orbit we still continue the family towards the alpha particle. This evolution is shown in Figure 6e. It is very important to point out that for $z \in (0.233, 0.591)$ they are stable. They are also stable for $z < 0.16$, but they are small orbits rather near the alpha particle.

Stable Halo orbits have two normal frequencies, besides its proper frequency. According to KAM theory ([1] and [13]), around each Halo orbit, there are a two parameter Cantorian family of 3D invariant tori. This family of tori can be labeled with three parameters: one for the corresponding periodic Halo orbit and two additional for the amplitudes with respect to that Halo orbit. The frequencies, generically, varies when moving these parameters. The family of 3D invariant tori is not a continuous family, it is a Cantor set and there are gaps between the tori. An electron orbiting in one of these gaps may escape as consequence of the Arnold's diffusion [2]. However, the time to escape would be certainly very long [8]. So, there is a subset of the phase space around the stable Halo orbits where an electron may probably remain for long time. Sometimes, such subsets are said effectively stable.

Finally, we want to comment that the 3D invariant tori can be computed using the numerical method described in [19] or semi-analytically using the Lindstedt-Poincaré method as in [11]. But, this computation is out of the scope of this article.

7 Regularization of the electron–alpha collision

To study numerically the bounded orbits in the vicinity of the alpha particle, it is convenient to regularize the electron–alpha collision. The singularity of the muon does not affect numerical calculations since it is a repulsive singularity.

In the planar case, i.e., for two degrees of freedom this is easily done through the Levi–Civita procedure. However, the three degrees of freedom case is much more involved since in this case the extension of the Levi–Civita procedure, requires a four degrees of freedom configuration with one constraint. In that case, it is necessary to use the Kustaanheimo-Stiefel transformation ([22] and [9]). Here, we shall deal only with the planar case.

We make a translation to bring the alpha particle to the origin, $\bar{x} = x - x_1$, so that Hamiltonian (20) becomes (calling $\bar{x}$, x again):

$$\bar{H} = \frac{1}{2}(p_x^2 + p_y^2) + yp_x - (x + x_1)p_y + \bar{\mu}\left[\frac{1}{(x^2+y^2)^{1/2}} - \frac{1}{2((x-1)^2+y^2)^{1/2}}\right]. \qquad (31)$$

We now apply the change of variables, known as Levi–Civita transformation, given by:

$$\begin{pmatrix} x \\ y \end{pmatrix} = \begin{pmatrix} \hat{x} & -\hat{y} \\ \hat{y} & \hat{x} \end{pmatrix} \begin{pmatrix} \hat{x} \\ \hat{y} \end{pmatrix}, \qquad (32)$$

the induced conjugate momenta transformation being

$$\begin{pmatrix} p_x \\ p_y \end{pmatrix} = \frac{2}{\hat{r}^2} \begin{pmatrix} \hat{x} & -\hat{y} \\ \hat{y} & \hat{x} \end{pmatrix} \begin{pmatrix} \hat{p}_x \\ \hat{p}_y \end{pmatrix}, \qquad (33)$$

where $\hat{r}^2 = (\hat{x}^2 + \hat{y}^2) = r = (x^2 + y^2)^{1/2}$. To complete the regularizing procedure it is also necessary a change of time scale, given by

$$d\hat{\tau} = \frac{4\, d\tau}{r}\ . \tag{34}$$

Using (32), (33) and (34) in $\hat{H}(\hat{\mathbf{q}}, \hat{\mathbf{p}}) = \frac{r}{4}(\bar{H}(\hat{\mathbf{q}}, \hat{\mathbf{p}}) + p_0)$, the regularized Hamiltonian is (suppressing hats):

$$\begin{aligned} H = \quad & \frac{p_0}{2}\frac{(x^2+y^2)}{2} + \frac{1}{2}(p_x^2+p_y^2) + \frac{1}{2}(x^2+y^2)(yp_x - xp_y) \\ & - \frac{x_1(yp_x + xp_y)}{2} + \frac{\bar{\mu}(x^2+y^2)}{8((x^2+y^2)^2 - 2(x^2-y^2)+1)^{1/2}}. \end{aligned} \tag{35}$$

The regularized equations of motion are:

$$\begin{aligned} \dot{x} &= p_x + \frac{y}{2}\left(r^2 - x_1\right)\ , \\ \dot{y} &= p_y - \frac{x}{2}\left(r^2 + x_1\right)\ , \\ \dot{p}_x &= -x(c + yp_x - xp_y) + p_y\frac{r^2+x_1}{2} - \frac{\bar{\mu}x}{4R}\left(1 - \frac{r^2(r^2-1)}{R^2}\right)\ , \\ \dot{p}_y &= -y(c + yp_x - xp_y) - p_x\frac{r^2-x_1}{2} - \frac{\bar{\mu}y}{4R}\left(1 - \frac{r^2(r^2+1)}{R^2}\right)\ , \end{aligned} \tag{36}$$

being $R = (r^4 - 2(x^2-y^2)+1)^{1/2}$, $r^2 = x^2+y^2$ and $c = p_0/2 = -\bar{h}/2$, where $\bar{h}$ is the chosen value of the energy leaf of $\bar{H}$.

7.1 Numerical Results

The Levi–Civita transformation takes the saddle–center to the y axis and create, due to its double covering, another saddle–center at $-y$, as if we had two muons on the y axis.

As expected, the regularization allows a comfortable numerical work. The first thing we point out is the fact that chaotic region is fairly large even for values of the energy far from the open *zvc*. We show in Figures 7 to 9 the Poincaré section defined by $y = 0$, $\dot{y} < 0$, i.e., $p_y < 0$. The initial conditions were chosen in the variables just before the regularizing transformation with the alpha particle at the origin. This is cumbersome but it helps to keep track of the original physical problem. In Figure 7, in Levi-Civita variables, we can see the chaotic behavior spreading in the outer region of the section for energies greater than $E = -110.0$.

In Figure 8 we show the same section shown in Figure 7 in physical variables. These are obtained from the section on Levi-Civita variables by applying the inverse transformation. To be able to show the sections of retrograde and direct motion in the same figure we change the sign of the x variable for the direct orbits and they are shown on the left hand side of the figures. The sections for the direct orbits show that they get completely chaotic before the retrograde ones. The retrograde orbits, on the left of the figure, stay on KAM tori for

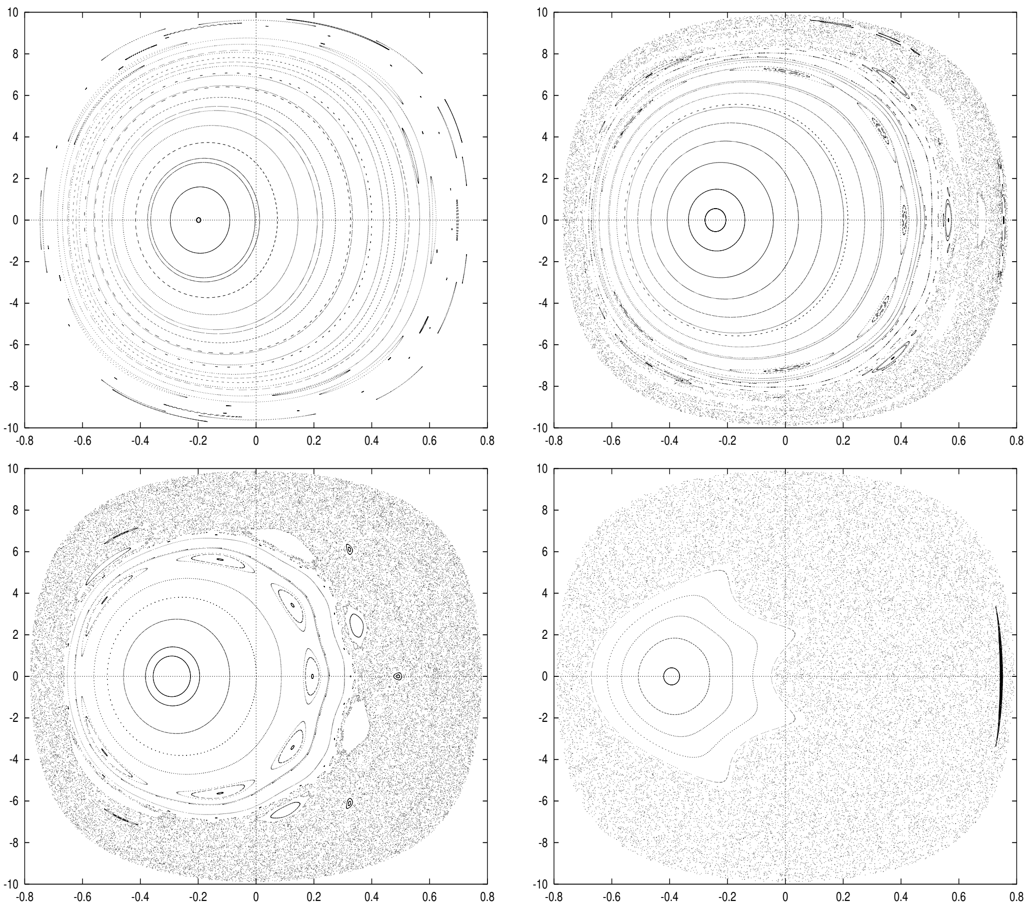

Figure 7: Poincaré section $y = 0, p_y < 0$ in Levi-Civita variables. Left to right, top to bottom: $-E = 120.0$, 90.0, 70.0 and 50.0, respectively. The chaotic zone increases with increasing energy, and KAM tori survive only in the left of the section.

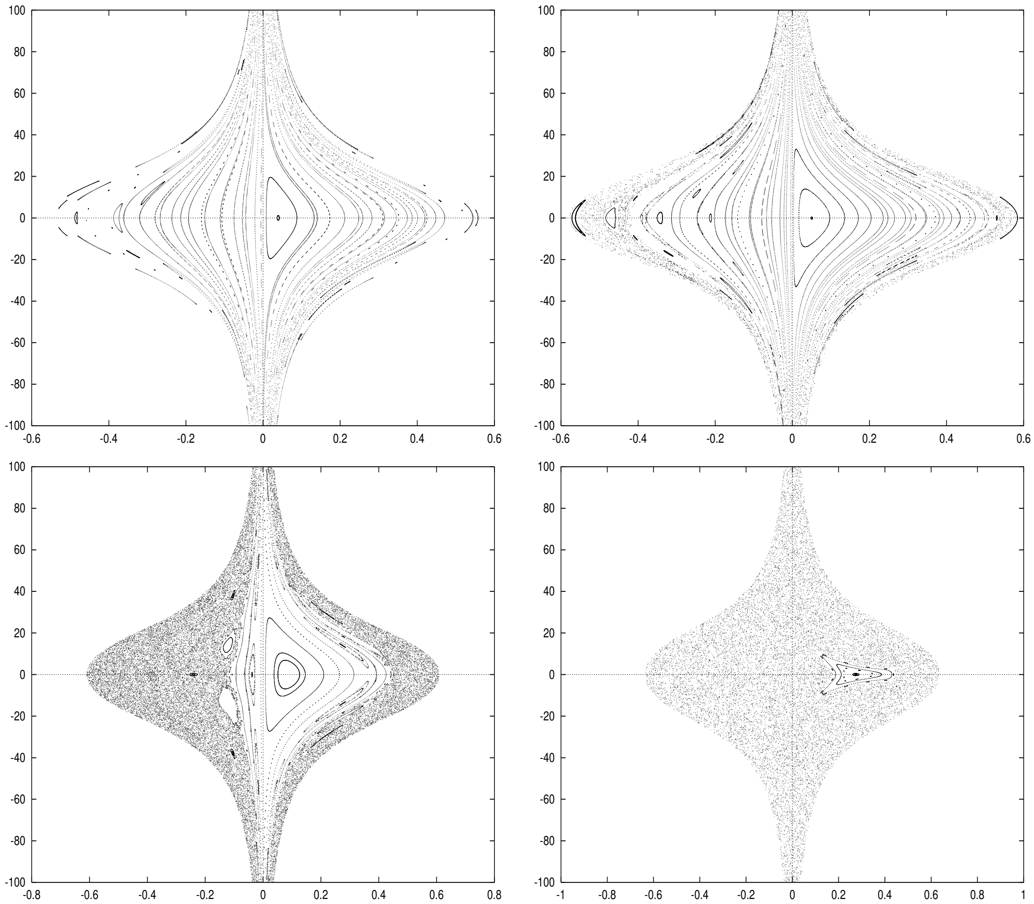

Figure 8: Left to right, top to bottom: Poincaré section $y = 0, p_y < 0$ in physical variables for $-E = 120.0$, 100.0, 70.0 and 38.0. The right hand side represents retrograde orbits while the left hand side are direct orbits of the electron.

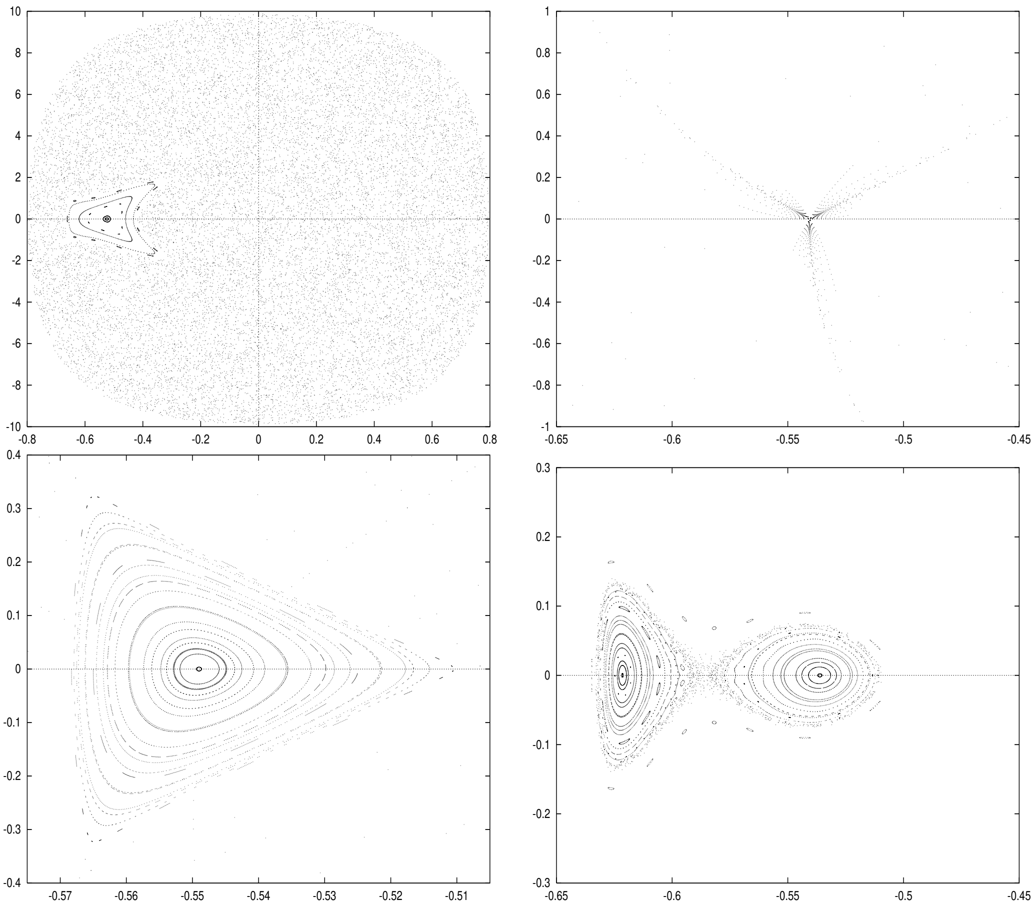

Figure 9: Same as Figure 7. The KAM curves are all retrograde. Left to right, top to bottom a) $E = -38.0$; b) $E = -37.0$, note that the triangular KAM tori structure collapses to an unstable orbit; c) $E = -36.5$, the triangular structure reappears inverted; d) $E = -34.5$.

a certain range of energy higher than the energy of the saddle-center, i.e, after the opening of the *zvc*. This is shown in Figure 9 in Levi-Civita variables. Before the *zvc* open, the triangular shaped KAM region is inverted (Figure 9c), after collapsing (Figure 9b), and subsists after the *zvc* open. In Figures 10a and 10b we show a Lagrangian projection of this final KAM region for $E = -33.8$ for both physical and Levi–Civita variables. The details of the tiny islands of the Poincaré section are shown in physical variables in 10c and 10d. There is no persistent KAM region as in the Hill problem [20].

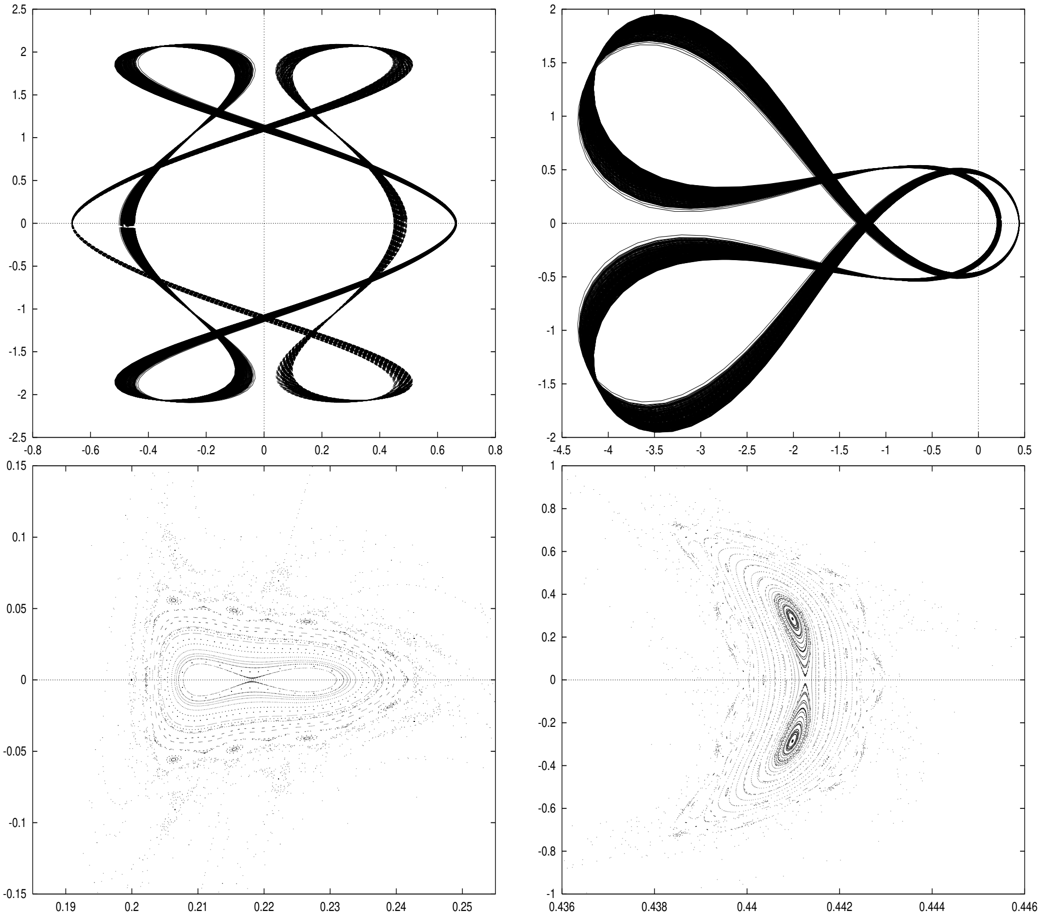

Figure 10: The small KAM zone for $E = -33.8$ when the fixed points in the Poincaré map of figure 9d have bifurcated. Projections on the configuration space in: a) Levi– Civita variables; b) Physical variables; c) and d) details of the Poincaré section in physical variables.

Another important point, is the existence of sets of periodic orbits with the same rotation number, stemming from the same rational tori. A good example appears at $E = -100.0$. Note that there two sets of island with rotation number 1/3. This is another interesting example of an unusual case of the Poincaré–Birkhoff theorem. The same phenomena can be observed in the case of the Hill problem [20]. In that problem the main case was a set of four periodic orbits with winding number 1/3. In neither case we have investigated this phenomena deeply.

8 Final Comments

We have not yet seen a full treatment of the muonic helium as we present in this paper, and we believe it is a contribution towards the understanding of its classical dynamics. The equilibrium configuration and the stable Halo periodic orbits are certainly an unknown interesting feature of the muonic helium shown in this paper. Therefore, we believe it might be useful in semi–classical studies of muonic and other helium–like atoms.

Acknowledgements

We are very grateful to Alejandro López–Castillo for invaluable discussions. M.A. Andreu wishes to acknowledge the hospitality of the dept. of Matemàtica Aplicada I, Universitat Politèctina de Catalunya (Barcelona, Spain).

References

[1] Arnol'd V.I.: *Proof of a theorem of A.N. Kolmogorov on the persistence of quasi-periodic motions under small perturbations of the Hamiltonian*, Russ. Math. Surveys, 18:5, pp. 9–36 (1963).

[2] Arnol'd V.I.: *Instability of dynamical systems with several degrees of freedom*, Sov. Math. Dokl. 5 581-5, (1964).

[3] Benvenuto, F., Casati, G., Shepelyansky, D.L.: *Chaos in a quasiclassical hadronic atom*, Physical Review A, 53-5, 737-743, (1993)

[4] Breakwell J.V., Brown J.V.: *The 'halo' family of 3-dimensional periodic orbits in the Earth-Moon restricted 3-body problem*, Celestial Mechanics 20, 389-404 (1979).

[5] López–Castillo A., *Hydrogen Molecule as a Classical Restricted Four-Body Problem*, Phys.Rev.Lett.,77 (22), 4516-19, (1996).

[6] López–Castillo A., de Aguiar M.A.M, Ozorio de Almeida A.M. J.Phys.B 29,197 (1996).

[7] López–Castillo A.,*Nonlinear dynamics of the hydrogen molecule*, Phys.Rev.A 58 (2),(1998).

[8] Delshams A., Gutiérrez P.: *Effective stability and KAM theory*, J. Diff. Eqns. 128, 415-90 (1996).

[9] Deprit A., Elipe A., Ferrer S.: *Linearization: Laplace vs. Stiefel*, Celestial Mechanics and Dynamical Astronomy 58, 151-201 (1994).

[10] Flothmann E. and Welge K.H. *Crossed hydrogen atom and the three-body Sun-Earth-Moon problem*, Phys.Rev.A 54 (3),1884-88 (1996).

[11] Gómez G., Masdemont J., Simó C.: *Quasihalo orbits associated with libration points*, Journal of the Astronautical Sciences (to appear).

[12] Gutzviller M.C., *Chaos in Classical and Quantum Mechanics* (New York: Springer) - (1990).

[13] Jorba À., Villanueva J.: *On the persistence of lower dimensional invariant tori under quasi-periodic perturbations*, Journal of Nonlinear Science, Vol. 7, pp. 427-473 (1997).

[14] Marchal C.: *The Three-Body Problem*, Elsevier (1990).

[15] Schaffner J., Dover C.B., Gal A. Greiner C. and Stoker H.: *Strange Hadronic Matter*, 71 (9) 1328-1331 (1993).

[16] Osório de Almeida, A.M. *Hamiltonian Systems: Chaos and Quantization*, Cambridge Univertiy Press, (1988).

[17] Siegel C., Moser J.K.: *Lectures on Celestial Mechanics*, Springer-Verlag, New York (1971).

[18] Simó C.: *Analytical and numerical computation of invariant manifolds.* In D. Benest et C. Froeschlé, editors, *Modern methods in celestial mechanics*, pag. 285-330, Editions Frontières (1990).

[19] Simó C.: *Effective Computations in Hamiltonian Dynamics*, in *Cent ans après les Méthodes Nouvelles de H. Poincaré*, Société Mathématique de France, 1–23, (1996).

[20] Simó C., Stuchi T.J.: *Central stable/unstable manifolds and the destruction of KAM tori in the planar Hill problem*, (to appear in Physica D).

[21] Solov'ev, E.A.:*Quasiclassical perturbation theory for the helium atom and heliumlike ions*, Sov.Phys.JETP **62** (6), ll48-1154, (1986).

[22] Stiefel E., Schiefele G.: *Linear and Regular Celestial Mechanics*, New York Heidelberg Berlin, Springer-Verlag (1971).

[23] Stoer J., Bulirsch R.: *Introduction to numerical analysis*, Springer-Verlag (1980).

[24] Szebehely V.: *Theory of orbits*, Academic Press, New York (1967).

[25] Yamamoto T. and Kaneko K., *Helium atom as a classical three body problem* Phys.Rev.Lett.70-13, 1928 (1993).

[26] D. Wintgen, K. Richter and G. Tanner, Chaos vol 2, 19-, (1992).